

# The $B \rightarrow X_s \gamma\gamma$ rare decay

L. Reina<sup>a</sup>, G. Ricciardi<sup>b</sup>, A. Soni<sup>a</sup>

<sup>a</sup>Physics Department, Brookhaven National Laboratory,  
Upton, NY 11973

<sup>b</sup>Dipartimento di Scienze Fisiche, Università degli Studi di Napoli,  
and I.N.F.N., Sezione di Napoli,  
Mostra d'Oltremare, Pad. 19, I-80125 Napoli, Italy

## Abstract

The rare decay  $B \rightarrow X_s \gamma\gamma$  is studied in the Standard Model (SM) and in two different versions (Model I and Model II) of the Two Higgs Doublet Model (2HDM). In the SM the branching ratio into *hard photons* is about  $1 \times 10^{-7}$  and can be appreciably different in the 2HDM. We also introduce a forward-backward asymmetry which gives an additional handle to discriminate different models.

## 1 Introduction

Intense experimental effort is being directed to B-physics. Several new facilities are on the horizon. There are, of course, the  $e^+e^-$  based symmetric and asymmetric B-factories at Cornell, KEK and SLAC, in addition to LEP II. Progress is also being made in the hadronic environment at HERA-B and there are some plans for TEV-B and far into the future, LHC-B. Indeed it is useful to recall that in the case of the kaon some of the branching ratios currently being measured have reached the  $10^{-10}$  level. It should then be clear that in B-physics too, the experimental activity is likely to continue to flourish well beyond the presently attainable branching ratios of about  $10^{-5}$ .

Amongst the rare decays the flavor changing decays of the B meson are of special interest, in particular those driven by the electroweak (EW) penguins, due to their relative cleanliness and to their sensitivity to new physics [1]. In this category, the two decays that have dominated the discussion for over a decade are  $b \rightarrow s\gamma$  and  $b \rightarrow sl^+l^-$ . It is useful to recall that the inclusive branching ratio for  $b \rightarrow s\gamma$  has been measured at CLEO to be [2]

$$Br(B \rightarrow X_s \gamma)^{\text{exp}} = (2.32 \pm 0.51 \pm 0.29 \pm 0.32) \times 10^{-4} \quad (1)$$

and a Next-to-Leading Order calculation of the same now exists [3–6]. The result [4]:  $Br(B \rightarrow X_s \gamma)^{\text{th}} = (3.28 \pm 0.33) \times 10^{-4}$  indicates agreement of the SM prediction with the CLEO measurement within  $2\sigma$ . As far as  $b \rightarrow sl^+l^-$  is concerned, the non-resonant part of  $B \rightarrow X_s \mu^+ \mu^-$  has been predicted to give [7]:  $Br(B \rightarrow X_s \mu^+ \mu^-)_{\text{NR}} = (5.7 \pm 0.9) \times 10^{-6}$ , while the existing upper bound on this decay mode from DØ is now being updated to [8]

$$Br(B \rightarrow X_s \mu^+ \mu^-) \leq 3.2 \times 10^{-5} , \quad (2)$$

less than one order of magnitude away from the theoretical prediction.

Our focus in this paper will be on a related mode:  $b \rightarrow s\gamma\gamma$  which is of the same order in the EW couplings as  $b \rightarrow sl^+l^-$  and is also of considerable interest. We will extend earlier works on this process and study it in the SM and in one of its most popular extensions, namely the 2HDM. The calculation of  $b \rightarrow s\gamma\gamma$  in the SM at the lowest order in the EW interactions and without QCD corrections gives a branching ratio of about  $10^{-7}$ , therefore in the ballpark of the rare B decays that should become accessible at the future B-meson facilities. Furthermore, we will introduce a forward-backward asymmetry which should be less sensitive to QCD corrections than the branching ratio and should also constitute a useful probe of the theory.

## 2 The $b \rightarrow s\gamma\gamma$ decay in the Standard Model

The decay  $B \rightarrow X_s \gamma\gamma$ <sup>1</sup> can be studied to a very good approximation in terms of the quark level decay  $b \rightarrow s\gamma\gamma$  [9]. The total amplitude for the quark level process can be written as [10–12]

$$A(b \rightarrow s\gamma\gamma) = -i \frac{\alpha_e G_F}{\sqrt{2}\pi} \epsilon_\mu(k_1) \epsilon_\nu(k_2) \bar{u}(p_s) T^{\mu\nu} u(p_b) , \quad (3)$$

where  $\alpha_e$  is the electromagnetic fine structure constant,  $G_F$  the Fermi coupling constant,  $p_b$  and  $p_s$  denote the momenta of the incoming and outgoing quarks and  $\epsilon_\mu(k_1)$  and  $\epsilon_\nu(k_2)$  are the polarization vectors of the two photons. The tensor  $T^{\mu\nu}$  is derived from the calculation of the Feynman diagrams of Fig. 1, when we sum over the three possible flavors of quarks that run in the penguin loop

$$T^{\mu\nu} = \sum_{i=u,c,t} \lambda_i T_i^{\mu\nu} = \lambda_u (T_u^{\mu\nu} - T_c^{\mu\nu}) + \lambda_t (T_t^{\mu\nu} - T_c^{\mu\nu}) . \quad (4)$$

---

<sup>1</sup>The inclusive calculation presented here is applicable to  $B_u$ ,  $B_d$  and  $B_s$  with the corresponding multiparticle state ( $X_s$ ) having the flavors of  $\bar{s}u$ ,  $\bar{s}d$  and  $\bar{s}s$  respectively. Moreover our calculations can be readily adapted to the case of  $b \rightarrow d\gamma\gamma$  with obvious changes.

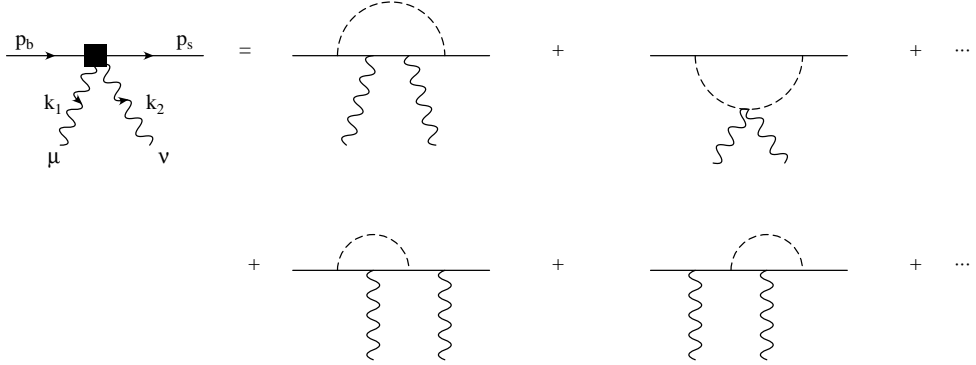


Figure 1: Examples of 1PI and 1PR contributions to the  $b \rightarrow s\gamma\gamma$  process. The dashed line represents a  $W$  (SM) or a charged scalar (2HDM).

Here  $\lambda_i = V_{ib}V_{is}^*$  is the CKM factor multiplying the loop diagrams with an internal  $i$ -quark and we have used the unitarity of the CKM matrix to obtain the last result. Even though  $\lambda_u \ll \lambda_t$ , for our purpose, as we will explain later, the first term cannot be neglected.

As we see from Fig. 1, both one-particle reducible (1PR) and one-particle irreducible (1PI) diagrams contribute to the process. We will follow the notation of Ref. [12] and write the total amplitude for the  $i$  flavor as

$$T_i^{\mu\nu} = T_{i,1\text{PI}}^{\mu\nu} + T_{i,1\text{PR}}^{\mu\nu} . \quad (5)$$

The 1PI contribution  $T_{i,1\text{PI}}^{\mu\nu}$  is then written as

$$T_{i,1\text{PI}}^{\mu\nu} = \frac{8}{9}\delta_3(z_i)I^{\mu\nu} , \quad (6)$$

where  $z_i = 2k_1 \cdot k_2 / m_i^2$  and  $\delta_3(z_i)$  is a function defined by [13]

$$\delta_3(z_i) = 1 + \frac{2}{z_i} \int_0^1 \frac{du}{u} \log [1 - z_i u(1 - u)] . \quad (7)$$

The tensor  $I^{\mu\nu}$  is given by<sup>2</sup>

$$I^{\mu\nu} = \left[ i\epsilon^{\mu\nu\xi\alpha} \gamma_\alpha \gamma_L (k_1 - k_2)_\xi + i \frac{k_{1\xi} k_{2\eta}}{k_1 \cdot k_2} (\epsilon^{\mu\xi\eta\alpha} k_1^\nu - \epsilon^{\nu\xi\eta\alpha} k_2^\mu) \gamma_\alpha \gamma_L \right] , \quad (8)$$

where we use the notation  $\gamma_{L,R} = (1 \mp \gamma_5)/2$ . On the other hand, the 1PR contribution has the form

$$T_{i,1\text{PR}}^{\mu\nu} = -i \frac{1}{3} F_2(x_i) W^{\mu\nu} (m_b \gamma_R + m_s \gamma_L) , \quad (9)$$

<sup>2</sup>We want to emphasize here that both Refs. [10] and [12] deal with the decay  $B_s \rightarrow \gamma\gamma$ . In that case one only needs to keep the first term in the  $I^{\mu\nu}$  tensor. This is not true for the inclusive  $B \rightarrow X_s \gamma\gamma$  decay.

where  $F_2(x_i)$  for  $x_i = m_i^2/M_W^2$  is the form factor of the magnetic dipole operator of the  $bs\gamma$  vertex [14], given by

$$F_2(x_i) = \frac{1}{36(1-x_i)^4} [-46 + 205x_i - 312x_i^2 + 175x_i^3 - 22x_i^4 + (36x_i^2 - 54x_i^3)\log(x_i))], \quad (10)$$

while the  $W^{\mu\nu}$  tensor is defined by the expression

$$\begin{aligned} W^{\mu\nu} = & - \left[ \left( \frac{p_s^\nu}{p_s \cdot k_2} - \frac{p_b^\nu}{p_b \cdot k_2} \right) \sigma(\mu, k_1) + \left( \frac{p_s^\mu}{p_s \cdot k_1} - \frac{p_b^\mu}{p_b \cdot k_1} \right) \sigma(\nu, k_2) \right] \\ & + \frac{i}{2} \left[ \left( \frac{1}{p_s \cdot k_2} - \frac{1}{p_b \cdot k_1} \right) \sigma(\nu, k_2) \sigma(\mu, k_1) + \left( \frac{1}{p_s \cdot k_1} - \frac{1}{p_b \cdot k_2} \right) \sigma(\mu, k_1) \sigma(\nu, k_2) \right]. \end{aligned} \quad (11)$$

The rate  $\Gamma(b \rightarrow s\gamma\gamma)$  can therefore be decomposed as the sum of a pure 1PR, a pure 1PI and an interference 1PR-1PI term, i.e.

$$\Gamma(b \rightarrow s\gamma\gamma) = \Gamma_{1\text{PR}} + \Gamma_{1\text{PI}} + \Gamma_{1\text{PR-1PI}}. \quad (12)$$

In order to obtain the total rate into *hard photons* we have to place suitable kinematical cuts and perform one dimensional integration numerically. We have also checked our results integrating over the phase space with a Montecarlo event generator.

Indeed the total rate and the relevance of each different contribution (1PR,1PI) depends appreciably on the kinematical cuts imposed. In order to isolate two *hard* photons, we demand that their energy is not too small and that they are not too collinear to each other and to the outgoing  $s$  quark. We thus require the energy of each photon to be larger than 100 MeV and that  $s_1 = (p_s + k_1)^2$ ,  $s_2 = (k_1 + k_2)^2$  and  $s_3 = (p_s + k_2)^2$  satisfy

$$s_1 \geq c m_b^2, \quad s_2 \geq c m_b^2, \quad s_3 \geq c m_b^2. \quad (13)$$

We take  $c = 0.01$  and  $c = 0.02$  to study the dependence on the cuts. Note that the resulting two photon invariant mass squared is at least one order of magnitude bigger than  $m_\pi^2$ . Furthermore all the angles are taken to be  $\gtrsim 20^\circ$ .

Our results are summarized in Table 1. These results are for pure EW penguins and do not include QCD corrections [15]. For  $m_t \simeq 175$  GeV, as in the  $b \rightarrow s\gamma$  case, QCD corrections are not likely to change the predictions of Table 1 dramatically. The branching ratios are calculated by normalizing to the semileptonic branching ratio, for which we have used the experimental value  $Br(B \rightarrow X_s e \nu_e) \simeq 0.11$ . We did not include QCD corrections in the semileptonic rate

		Br( $b \rightarrow s\gamma\gamma$ ) $\times 10^{-7}$				$A_{FB}$
		Total	1-Particle Reducible	1-Particle Irreducible	Interference	
SM		c=0.01				
		1.60	1.30	0.23	0.08	0.69
2HDM	tan $\beta$	0.5	0.23-14.67	0.003-14.70	0.23	-(0.26-0.003)
		1	0.23-1.26	0.01-0.96	0.23	-0.007-0.07
		10	1.57-1.59	1.26-1.29	0.23	0.07
Model I		0.5	2.19-16.67	1.87-16.17	0.23	0.09-0.27
		1	2.07-9.65	1.75-9.21	0.23	0.09-0.21
		10	2.03-7.76	1.71-7.34	0.23	0.09-0.18
2HDM	tan $\beta$	0.5	2.19-16.67	1.87-16.17	0.23	0.70-0.75
		1	2.07-9.65	1.75-9.21	0.23	0.70-0.74
		10	2.03-7.76	1.71-7.34	0.23	0.70-0.74
SM		c=0.02				
		1.33	1.02	0.23	0.08	0.64
2HDM	tan $\beta$	0.5	0.23-11.57	0.003-11.60	0.23	-(0.26-0.003)
		1	0.23-1.05	0.009-0.76	0.23	-0.007-0.07
		10	1.30-1.33	0.99-1.01	0.23	0.07
Model I		0.5	1.80-13.26	1.48-12.76	0.23	0.09-0.27
		1	1.70-7.71	1.38-7.23	0.23	0.09-0.21
		10	1.67-6.21	1.35-5.79	0.23	0.089-0.18
2HDM	tan $\beta$	0.5	1.80-13.26	1.48-12.76	0.23	0.66-0.71
		1	1.70-7.71	1.38-7.23	0.23	0.65-0.71
		10	1.67-6.21	1.35-5.79	0.23	0.65-0.70

Table 1: Values of branching ratio and forward-backward asymmetry obtained in the SM and in the 2HDM's (Model I and II), for two different values of the cut. In the 2HDM case we give a range of values corresponding to the variation of  $M_h$  between 100 GeV and 1 TeV.

either; for our purpose QCD effects are completely marginal here. For the numerical results we have used:  $m_t = 175$  GeV,  $m_c = 1.5$  GeV,  $m_u = 4.5$  MeV and  $m_b = 4.5$  GeV. However, we have checked the dependence of the results on  $m_c$  and  $m_u$ , allowing them to vary in the ranges  $1.2 < m_c < 1.8$  GeV and  $4.5 < m_u < 100$  MeV. We find that the dependence on  $m_u$  is totally negligible while the branching ratio varies up to 15 – 20% within this very conservative range of  $m_c$ . For  $m_s$  we have made the following distinction: in the calculation of the quark decay amplitude we have taken the current quark mass,  $m_s = 150$  MeV, while in the integration over the phase space, in order to respect the kinematics of the decay as closely as we can, we have used the  $K$  meson mass and taken approximately  $m_s = 450$  MeV. Again this assumption does not affect the results by more than 8% in any case. As far as the CKM matrix elements are

concerned, we have used:  $V_{cs} \simeq V_{tb} \simeq 1$ ,  $V_{us} \simeq 0.22$ ,  $|V_{ts}| \simeq |V_{cb}| \simeq 0.04$  and  $|V_{ub}/V_{cb}| \simeq 0.08$ .

In Table 1 we also give results separately due to 1PR, 1PI and due to their interference. As we can see, the role played by the 1PR and 1PI contributions varies a little with the different cuts imposed. With mild cuts, the 1PR contribution is dominant, due to the divergent behavior of the amplitude for  $s_2 \rightarrow 0$ . This divergent behavior is caused by the presence of both infrared ( $E_\gamma \rightarrow 0$ ) and collinear ( $\cos \theta_{\gamma\gamma} \rightarrow 0$ ) divergencies, which, for sure, would cancel in a complete analytical calculation when virtual photon corrections at the same order in  $\alpha_e$  are also included. Experimentally, if one of the two photons in  $b \rightarrow s\gamma\gamma$  decay is emitted with very low energy and/or at a very small angle with respect to the other photon, it becomes difficult to distinguish the event from a  $b \rightarrow s\gamma$  decay. Therefore we exclude this region of the phase space by imposing the cuts mentioned earlier. This tends to suppress the 1PR contribution compared to the 1PI one.

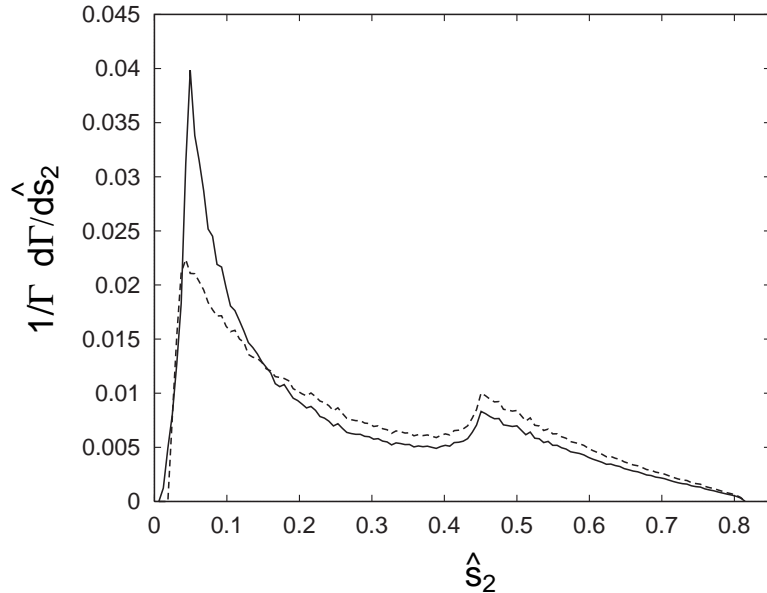


Figure 2: The normalized distribution  $1/\Gamma \cdot d\Gamma/d\hat{s}_2$  versus  $\hat{s}_2 = s_2/m_b^2$  in the SM for two values of the cut parameter:  $c = 0.01$  (solid) and  $c = 0.02$  (dashed). Also,  $\langle \hat{s}_2 \rangle = 0.25, 0.28$  for  $c = 0.01$  or  $c = 0.02$  respectively.

Moreover, the analytical expressions of the 1PR and 1PI terms in Eqs. (5)-(11) are such that the light quarks mainly contribute to the 1PI part and the heavy quarks to the 1PR one. This is due to the analytical behavior of the coefficient functions  $\delta_3(z_i)$  and  $F_2(x_i)$  (see Ref. [12] for a plot of these functions). The physical reason for this is that, when the top quark runs in the loop of the penguin diagram for  $b \rightarrow s\gamma\gamma$  (both in the 1PR and in the 1PI diagrams), the amplitude for the decay is very well approximated by the amplitude for the emission of a

brehmstrahlung photon off the  $s$  quark leg. Indeed by this reasoning, the authors of Ref. [5] were able to get the right expression for the top contribution using Low's theorem [16]. Thus the higher the kinematical cuts imposed to reduce the  $s$  quark brehmstrahlung events, the higher the relevance of the light quark contribution (i.e. 1PI) to the total amplitude. For this reason we retained in Eq. (4) both the  $\lambda_t$  and the  $\lambda_u$  terms, in order to have the light quark dependence fully under control.

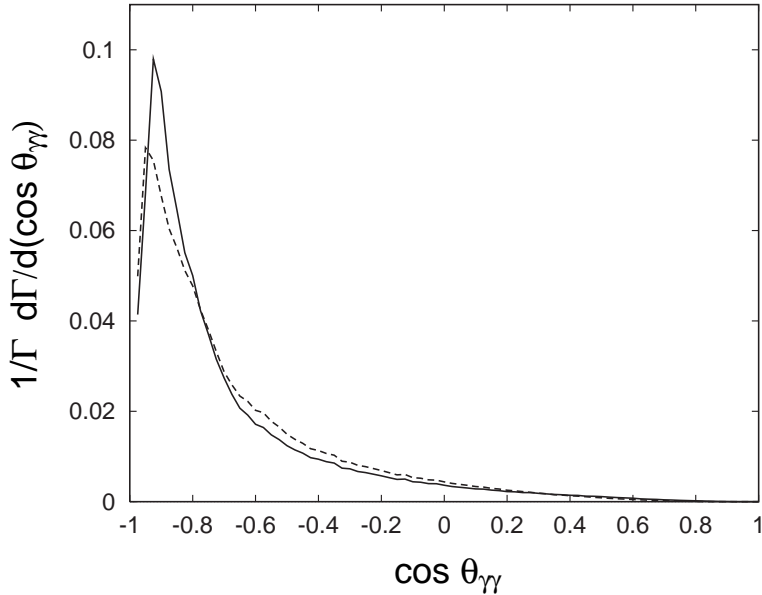


Figure 3: The normalized distribution  $1/\Gamma \cdot d\Gamma/d(\cos \theta_{\gamma\gamma})$  versus  $\cos \theta_{\gamma\gamma}$  in the SM for two values of the cut parameter:  $c = 0.01$  (solid) and  $c = 0.02$  (dashed). Also,  $\langle \cos \theta_{\gamma\gamma} \rangle = -0.70, -0.68$  for  $c = 0.01$  or  $c = 0.02$  respectively.

In Fig. 2 and 3 we present the results for two different distributions:  $d\Gamma/d\hat{s}_2$  ( $\hat{s}_2 = s_2/m_b^2$ ) and  $d\Gamma/d(\cos \theta_{\gamma\gamma})$ , where  $\theta_{\gamma\gamma}$  is the angle between the two photons, for the two sets of cuts<sup>3</sup>. As we can see the kinematics of the process is such that the  $s$  quark tends to be emitted with rather high energy, compensated by the harder of the two photons, while the less energetic photon tends to go in the direction of the  $s$  quark. This topology is typical of a brehmstrahlung event of the  $s$  quark and in fact it gets enhanced when we choose milder cuts on the energies and on the angles.

Although the  $b \rightarrow s\gamma\gamma$  process is higher order in  $\alpha_e$  and rarer than  $b \rightarrow s\gamma$ , it does allow one to introduce an additional feature that may be a useful probe of the dynamics of the decay, namely a forward-backward asymmetry, defined as

<sup>3</sup>We observe that the behavior of  $1/\Gamma \cdot d\Gamma/d\hat{s}_2$  around  $\hat{s}_2 \simeq 0.45$  (i.e.  $s_2 \simeq 9 \text{ GeV}^2$ ) corresponds, for  $m_c = 1.5 \text{ GeV}$ , to  $s_2 = 4m_c^2$ , i.e. to the physical threshold for an on-shell  $c\bar{c}$  pair.

$$A_{\text{FB}} = \frac{\Gamma(\cos \theta_{s\gamma} \geq 0) - \Gamma(\cos \theta_{s\gamma} < 0)}{\Gamma(\cos \theta_{s\gamma} \geq 0) + \Gamma(\cos \theta_{s\gamma} < 0)} , \quad (14)$$

where  $\theta_{s\gamma}$  is the angle between the  $s$  quark and the softer photon. Indeed, due to the identical nature of the two photons, this is the only non-trivial angle we can think of to study a forward-backward asymmetry. We recall that a forward-backward asymmetry has also been found to be useful in the study of the  $b \rightarrow sl^+l^-$  decay [17]. Our results are summarized in Table 1, for two different values of the cuts. In passing, we must remark that we expect  $A_{\text{FB}}$  to be less affected by QCD corrections than the branching ratio.

### 3 The $b \rightarrow s\gamma\gamma$ decay in the Two Higgs Doublet Model

We want now to consider the  $b \rightarrow s\gamma\gamma$  decay in the context of a 2HDM with no flavor changing neutral currents allowed at the tree level, i.e. Model I and Model II, in which the up and down type quarks couple respectively to the same or to two different Higgs doublets.

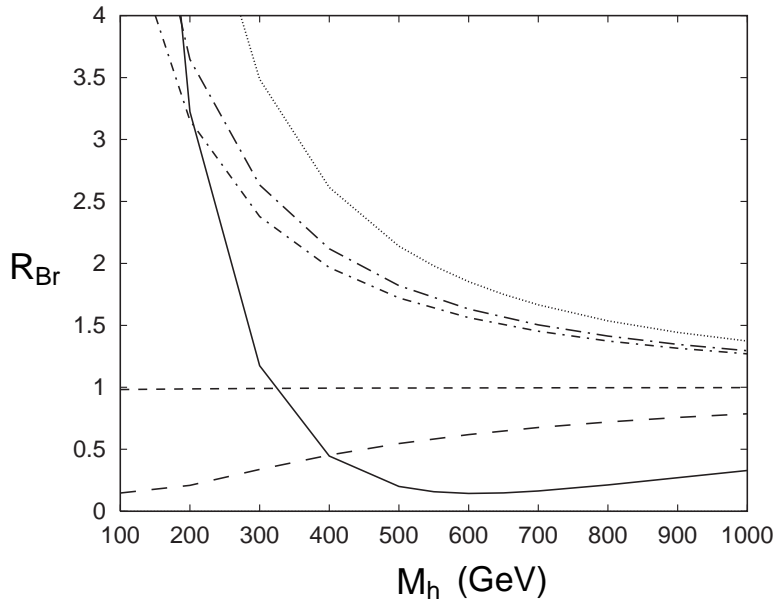


Figure 4: The ratio  $R_{\text{Br}}$  as a function of the charged scalar mass  $M_h$ , for different values of  $\tan \beta$  in Model I (solid:  $\tan \beta = 0.5$ ; long-dashed:  $\tan \beta = 1$ ; short-dashed:  $\tan \beta = 10$ ) and Model II (dotted:  $\tan \beta = 0.5$ ; long-dash-dot:  $\tan \beta = 1$ ; short-dash-dot:  $\tan \beta = 10$ ). The curves correspond to the cut parameter  $c = 0.01$ .

The physical charged scalar field contributes to the  $b \rightarrow s\gamma\gamma$  decay via a new class of Feynman diagrams in which the  $W$  boson is replaced by the charged scalar. However, the only important contributions are those with a top quark in the penguin loop, because of the

proportionality of the scalar-fermion coupling to the fermion mass<sup>4</sup>. Therefore, the amplitude for  $b \rightarrow s\gamma\gamma$  in Model I and Model II will be given by Eq. (4) where we only modify  $T_{t,1\text{PR}}^{\mu\nu}$  to include the new form factor [18]

$$F_2^{\text{2HDM}}(y_t) = \frac{y_t}{36(1-y_t)^4} \left\{ \xi^2 [7 - 12y_t - 3y_t^2 + 8y_t^3 + 6y_t(2 - 3y_t) \log y_t] + 6\xi\xi'(1-y_t) [3 - 8y_t + 5y_t^2 + 2(2 - 3y_t) \log y_t] \right\}, \quad (15)$$

where  $y_t = (m_t/M_h)^2$  and  $M_h$  denotes the mass of the charged scalar. Moreover we have used the notation<sup>5</sup>:  $\xi = v_1/v_2 = 1/\tan\beta$  and respectively

$$\begin{aligned} \xi' &= \xi && \text{in Model I} \\ \xi' &= -\frac{1}{\xi} && \text{in Model II} . \end{aligned} \quad (16)$$

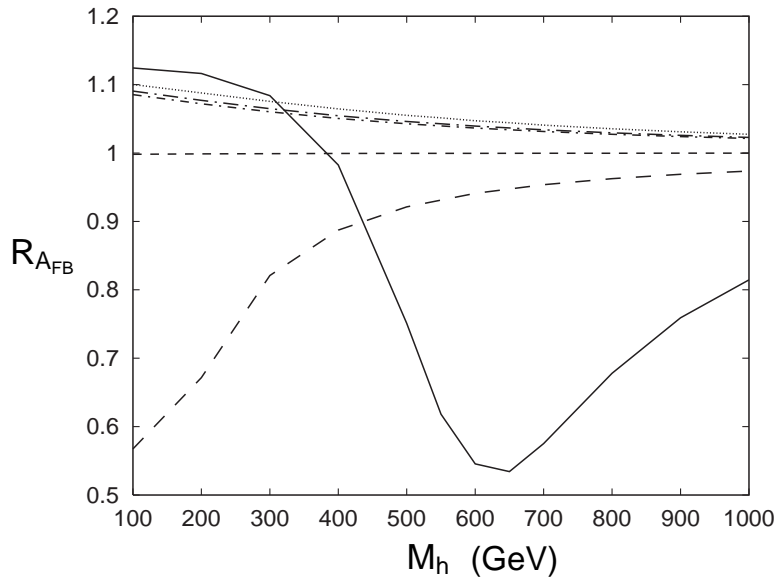


Figure 5: The ratio  $R_{A_{\text{FB}}}$  as a function of the charged scalar mass  $M_h$ , for different values of  $\tan\beta$  in Model I (solid:  $\tan\beta = 0.5$ ; long-dashed:  $\tan\beta = 1$ ; short-dashed:  $\tan\beta = 10$ ) and Model II (dotted:  $\tan\beta = 0.5$ ; long-dash-dot:  $\tan\beta = 1$ ; short-dash-dot:  $\tan\beta = 10$ ). The curves correspond to the cut parameter  $c = 0.01$ .

Summary of comparisons is given in Table 1 and in Figs. 4-5. In these two figures the differences between the 2HDM's and the SM are parametrized in terms of the two ratios

<sup>4</sup>This means that the new contribution to the  $m_c$  and  $m_u$ -dependent terms in the amplitude are much smaller than the corresponding SM contributions, both 1PR and 1PI.

<sup>5</sup>Note that the notation of Ref. [18] for Model I and Model II is the reverse of ours.

$$R_{\text{Br}} = \frac{Br(B \rightarrow X_s \gamma \gamma)^{\text{2HDM}}}{Br(B \rightarrow X_s \gamma \gamma)^{\text{SM}}} \quad \text{and} \quad R_{\text{A}_{\text{FB}}} = \frac{A_{\text{FB}}^{\text{2HDM}}}{A_{\text{FB}}^{\text{SM}}} \quad (17)$$

both for Model I and Model II. For illustrative purposes we consider three values of  $\tan \beta$ , namely  $\tan \beta = 0.5, 1, 10$  and we allow  $M_h$  to range between 100 GeV and 1 TeV. In this regard we should recall that  $M_h$  is also somewhat constrained by the experimental measurement of  $Br(B \rightarrow X_s \gamma)$  (see Eq. (1)). The present situation seems to indicate that  $M_h \gtrsim 200 - 300$  GeV. However both experiment and theory still have an appreciable error. Therefore we are tentatively considering  $M_h \geq 100$  GeV. The upper bound of 1 TeV is, of course, dictated by the requirement of a weak-coupled scalar sector. For Figs. 4 and 5 we also fixed  $c = 0.01$  and kept the other cuts on  $E_\gamma$  and on the angles as before. In fact a different value of the cut parameter (e.g.  $c = 0.02$ ) does not change the curves in Figs. 4 and 5 significantly.

We can see that Model II gives always both a bigger branching ratio and a bigger asymmetry than the SM. However while the asymmetry is very close to the SM value, the branching ratio can be much larger than the SM one over a wide range of values of the scalar mass, especially for light  $M_h$ .

The behavior of Model I is quite different. Both the branching ratio<sup>6</sup> and the asymmetry may be bigger or smaller than the SM, over different ranges of  $M_h$  and for different values of  $\tan \beta$ . Moreover the relative importance of 1PR and 1PI contributions may be very different than in the SM, due to a cancellation between  $F_2^{\text{SM}}(x_t)$  and  $F_2^{\text{2HDM}}(y_t)$  for some particular values of  $M_h$  and  $\tan \beta$ . As we can see from Table 1, there are cases in which the 1PI contribution (i.e. mainly the light quark one) is dominant. It is also interesting to note how different values of  $\tan \beta$  imply a totally different behavior both of  $R_{\text{Br}}$  and of  $R_{\text{A}_{\text{FB}}}$  and they complement each other by giving substantial deviations from the SM in different regions of the  $M_h$  spectrum. For example, in the case of  $\tan \beta = 0.5$ , for light  $M_h$  the branching ratio gives a much larger deviation from the SM than the asymmetry, while for heavier  $M_h$ , even up to  $M_h \simeq 1$  TeV, the asymmetry can be more interesting, especially because the branching ratio is smaller than the SM one in this region. For  $\tan \beta = 1$ , on the other hand, both the branching ratio and the asymmetry are quite different from the SM for  $M_h \lesssim 500$  GeV.

This description has one obvious shortcoming, namely that QCD corrections are not included. However we do not think that the inclusion of QCD corrections in either the SM or in the 2HDM calculation should greatly change the important features that we have described above.

---

<sup>6</sup>A similar behavior was found in Ref. [19] for the  $b \rightarrow s \gamma$  decay.

## 4 Experimental Considerations

Our primary focus of course has been on the inclusive  $b \rightarrow s\gamma\gamma$  process. As always it is very difficult to make reliable predictions about exclusive channels. Nevertheless, some general remarks can be made. Unlike  $b \rightarrow s\gamma$ , for  $b \rightarrow s\gamma\gamma$  the pseudoscalar ( $K$  for  $B$ ,  $\eta$  and  $\eta'$  for  $B_s$ ) as well as the vector ( $K^*$  for  $B$  and  $\phi$  for  $B_s$ ) final states are both allowed. These single meson states are likely to be a large fraction, perhaps several tens of percents of the total  $B \rightarrow X_s\gamma\gamma$  sample. Since the inclusive branching fraction of charmless  $B$  events is roughly estimated to be about 1%, they are likely to provide the most important background. However it is useful to note that a very important characteristic of  $b \rightarrow s\gamma\gamma$  is that the photons carry off an appreciable fraction of the total energy, leaving the mean energy of the  $s$  quark to be around 1.7 GeV. Thus we expect these  $2\gamma$  events to be relatively clean with an average multiplicity substantially less than in charmless  $B$  events. This property should come in handy for separating the  $2\gamma$  *background* coming from the decay of  $\pi^0$ ,  $\eta$  and  $\eta'$  from amongst the multibody charmless  $B$  events. Another remarkable feature of the prompt  $b \rightarrow s\gamma\gamma$  signal is that the photons have a large opening angle ( $\langle \cos \theta_{\gamma\gamma} \rangle \simeq -0.7$ ), as is seen in Fig. 3. This is in sharp contrast to the  $2\gamma$ 's from decays of the  $\pi^0$ ,  $\eta$  or  $\eta'$ , which, as a rule, should have a much smaller opening angle.

## Acknowledgments

We thank David Atwood, Hubert Simma and Ed Yao for discussions. One of us (G.R.) acknowledges the warm hospitality of Brookhaven National Laboratory, during the first stage of this work. This research was supported in part by U.S. Department of Energy contract DE-AC-76CH0016 (BNL).

## References

- [1] For a review see, e.g., J. Hewett. “*Top ten models constrained by  $b \rightarrow s\gamma$* ”, published in the Proceedings of “Spin structure in high energy processes”, p. 463, Stanford, 1993.
- [2] R. Ammar *et al.*, CLEO Collaboration, Phys. Rev. Lett. **71** (1993) 674; M.S. Alam *et al.*, CLEO Collaboration, Phys. Rev. Lett. **74** (1995) 2885.
- [3] C. Greub, T. Hurth and D. Wyler, Phys. Lett. **B380** (1996) 385; Phys. Rev. **D54** (1996) 3350; hep-ph/9608449.

- [4] K.G. Chetyrkin, M. Misiak and M. Münz, hep-ph/9612313.
- [5] K. Adel and Y.-P. Yao, Mod. Phys. Lett. **A8** (1993) 1679; Phys. Rev. **D49** (1994) 4945.
- [6] B. Grinstein, R. Springer, and M. Wise, Nucl. Phys. **B339** (1990) 269; R. Grigjanis, P.J. O'Donnell, M. Sutherland and H. Navelet, Phys. Lett. **B213** (1988) 355; Phys. Lett. **B286** (1992) E, 413; G. Celli, G. Curci, G. Ricciardi and A. Viceré, Phys. Lett. **B325** (1994) 227, Nucl. Phys. **B431** (1994) 417; M. Misiak, Nuc. Phys **B393** (1993) 23; M. Ciuchini, E. Franco, G. Martinelli, L. Reina and L. Silvestrini, Phys. Lett. **B316** (1993) 127; Nucl. Phys. **B421** (1994) 41.
- [7] M. Misiak, Nucl. Phys. **B393** (1993) 23, Erratum, Nucl. Phys. **B439** (1995) 461; A.J. Buras and M. Münz, Phys. Rev. **D52** (1995) 186; O. Bäer, Diploma Thesis, LUM (1996).
- [8] A.J. Buras, Proceedings of the *28<sup>th</sup> International Conference on High Energy Physics*, Warsaw, Poland, 25-31 July 1996, hep-ph/9610461 and references therein.
- [9] I.I. Bigi, Proceedings of the “*1994 International Workshop on B-Physics*”, Nagoya, p. 391, Eds. A.I. Sanda and S. Suzuki, World Scientific, and references therein.
- [10] G.-L. Lin, J. Liu and Y.-P. Yao, Phys. Rev. **D42** (1990) 2314.
- [11] H. Simma and D. Wyler, Nucl. Phys. **B344** (1990) 283.
- [12] S. Herrlich and J. Kalinowski, Nucl. Phys. **B381** (1992) 501.
- [13] M.K. Gaillard and B.W. Lee, Phys. Rev. **D10** (1974) 897; E. Ma and A. Pramunida, Phys. Rev. **D24** (1981) 2476.
- [14] T. Inami and C.S. Lim, Prog. Th. Phys. **65** (1981) 297; Erratum, ibidem, 1772.
- [15] Work on QCD corrections, by the authors, is in progress and will be published elsewhere.
- [16] F.E. Low, Phys. Rev. **110** (1958) 974
- [17] A. Ali, T. Mannel and T. Morozumi, Phys. Lett. **B273** (1991) 505.
- [18] T.M. Aliev and G. Turan, Phys. Rev. **D48** (1993) 1176.
- [19] W.-S. Hou and R.S. Willey, Phys. Lett. **B202** (1988) 591; B. Grinstein *et al.*, Ref. [6].